Number of words in the manuscript: 5218 words

Number of figures: 4 figures

Decomposing the role of alpha oscillations during brain maturation

AUTHORS:

Marius Tröndle[1,2,*], Tzvetan Popov[1,2], Nicolas Langer[1,2]

AFFILIATIONS:

1: Department of Psychology, University of Zurich, Methods of Plasticity Research, Department of Psychology, University of Zurich, Zurich, Switzerland

2: University Research Priority Program (URPP) Dynamic of Healthy Aging, Zurich, Switzerland

CORRESPONDING AUTHOR(*):

Marius Tröndle

Methods of Plasticity Research

Department of Psychology

University of Zurich

Andreasstrasse 15

CH-8050, Zürich, Switzerland

E-mail: m.troendle@psychologie.uzh.ch

Tel.: +41 44 635 34 14

Abstract

During childhood and adolescence, the human brain undergoes various micro- and macroscopic changes. Understanding the neurophysiological changes within this reorganizational process is crucial, as many major psychiatric disorders emerge during this critical phase of life. In electroencephalography (EEG), a widely studied signal component are alpha oscillations (~8-13 Hz), which have been linked to developmental changes throughout the lifespan. Previous neurophysiological studies have demonstrated an increase of the alpha peak frequency and a decrease of alpha power to be related to brain maturation. The latter results have been questioned by recent developments in EEG signal processing techniques, as it could be demonstrated that aperiodic (non-oscillatory) components in the EEG signal conflate findings on periodic (oscillatory) changes, and thus need to be decomposed accordingly. We therefore analyzed a large, openly available pediatric dataset of 1485 children and adolescents in the age range of 5 to 21 years, in order to clarify the role of alpha oscillations and aperiodic signal components in this period of life. We first replicated previous findings of an increase of alpha peak frequency with age. Our results further suggest that alpha oscillatory power decreases with increasing age, however, when controlling for the aperiodic signal component, this effect inverted such as the aperiodic adjusted alpha power parameters significantly increase with advanced brain maturation, while the aperiodic signal component flattens and its offset decreases. Thus, interpretations of these oscillatory changes should be done with caution and incorporate changes in the aperiodic signal. These findings highlight the importance of taking aperiodic signal components into account when investigating age related changes of EEG spectral power parameters.

1. Introduction

Childhood and adolescence are critical stages of the human lifespan, in which the brain undergoes various and complex micro- and macroscopic changes (Giedd et al., 1999; Lebel, Walker, Leemans, Phillips, & Beaulieu, 2008). The typical emergence of some major mental illnesses during childhood and adolescence further indicates fundamental maturational reorganization. Epidemiologic studies indicate that 70% of all psychiatric disorders begin prior to age 24 (Kessler et al., 2005). It is therefore particularly important to understand these changes in brain structure and function, which are accompanied by neurophysiological changes. A substantial body of literature has emerged from the neurophysiological investigation of these changes using electroencephalography (EEG). Specifically, alpha oscillations have previously been linked to developmental changes throughout the lifespan (Klimesch, 1999). Alpha oscillations are generally defined as neural oscillations in a frequency range of around 8 to 13 Hz (Niedermeyer, 1999) and are the most studied phenomenon in the human EEG. These oscillations, typically observed in parietal and occipital electrodes (Markand, 1990), were previously linked to important cognitive abilities of daily life such as inhibition (Klimesch, 2012; Niedermeyer, 1999), attention (Foxe & Snyder, 2011; Klimesch, 2012) and memory retrieval (Klimesch, 1997). Alpha oscillations are commonly investigated in terms of their power (averaged amplitude in the defined range of alpha oscillations) and their peak frequency (i.e. the frequency position of the highest observed amplitude within the alpha range).

In brain maturation research, there is consistent evidence for a slowing of the individual alpha frequency in the age range of around 7 to 14 years (Cragg et al., 2011; Díaz de León, Harmony, Marosi, Becker, & Alvarez, 1988; Klimesch, 1999; Somsen, van't Klooster, van der Molen, van Leeuwen, & Licht, 1997). Concerning the amplitude of this alpha oscillation (i.e. alpha power), the evidence is less clear. Investigating developmental changes in absolute power, several studies observed a reduction of power with increasing age within childhood and adolescence (Díaz de León et al., 1988; Gasser, Verleger, Bächer, & Sroka, 1988; Harmony et al., 1995; Whitford et al., 2007) while some studies did not find this association (Clarke, Barry, McCarthy, & Selikowitz, 2001; Somsen et al., 1997). When alpha power is investigated relative to the overall power of the spectrum (i.e. relative alpha power), there is more consistency on an increase of alpha power with age within childhood and adolescence (Clarke et al., 2001; Cragg

et al., 2011; Díaz de León et al., 1988; Harmony et al., 1995; John et al., 1980; Somsen et al., 1997).

Recent developments in EEG methods reveal that previous studies on frequency band power may be confounded by an overlooked signal component: the aperiodic signal (Donoghue et al., 2020b). It is claimed, that the EEG power spectrum consists not only of an oscillatory (i.e. periodic) signal, but also of a non-oscillatory (i.e. aperiodic) signal, which are both superimposed in the measured spectra (see Figure 1). The aperiodic signal is characterized by its shape (1/f), as its amplitude decreases with higher frequencies f. In the past years, this signal gained increased attention by the research community. Its offset could be linked to the general spiking activity (Voytek & Knight, 2015), its slope to the temporal correlation of the underlying neural population (Miller, Sorensen, Ojemann, & den Nijs, 2009; Usher, Stemmler, & Olami, 1995). One of the methodological challenges in EEG spectral analysis is to accurately decompose the EEG power spectrum into aperiodic and oscillatory signals. A new publicly available algorithm, Fitting Oscillations One Over F (Donoghue et al., 2020b) performs this decomposition and allows the aperiodic signal to be incorporated into spectral EEG analysis. One previous study on brain maturation from childhood to adulthood used this algorithm and provided first evidence for a possible confound of the aperiodic signal and oscillatory power in the measured power spectrum (He et al., 2019). Using a cross sectional approach, the authors compared 24 young children to 24 adults. Although no age effects regarding alpha band power were reported, it could be shown that the aperiodic signal is flatter, and its intercept is decreased in adults compared to children. The authors additionally found decreased power in delta and theta band as well as increased power in the beta and gamma band in the adult sample compared to children. When adjusting power for the aperiodic signal, changes in delta, theta and gamma were not observable anymore. Due to the nature of the investigated sample, it remains unknown to what extent the periodic and aperiodic signal components develop from childhood to adolescents.

The present study aims to close this gap, by investigating alpha oscillatory parameters and aperiodic signal components during brain maturation, and how the adjustment for the aperiodic signal affects results found in alpha power parameters. To overcome limitations of previous studies, we analyzed the currently largest openly available pediatric EEG data set (N=1609), comprising children and adolescents in the range of 5 to 21 years. Periodic and aperiodic parameters were extracted based on well-established procedures (Donoghue et al., 2020b; Klimesch, 1999). Specifically, this implies extracting individual alpha peak frequency, total alpha peak power (i.e. absolute power) and total broadband power. Subsequently, these alpha

power indices were adjusted for the aperiodic signal components (i.e. aperiodic adjusted power) using the FOOOF algorithm. Additionally, the developmental trajectories of the aperiodic signal (i.e. slope and intercept) were investigated (see table 1 for an overview and description of all investigated parameters). All analyses were performed in a Bayesian regression framework (Bürkner, 2017). Based on previous literature, we hypothesize to replicate the finding of reduced total alpha power during brain maturation using this larger sample size. We further hypothesize that this relation is no longer observable when adjusting for the aperiodic signal. Additionally, we expected to replicate the decrease of the aperiodic intercept and the flattening of the aperiodic slope during brain maturation, as well as the slowing of the IAF.

2. Methods:

2.1. Dataset

For the purpose of this study, 1644 resting state EEG datasets were obtained from the Human Brain Network (HBN) project (Alexander et al., 2017). The HBN project by the Child Mind Institute is an ongoing initiative that aims at generating a freely available biobank of multimodal datasets of children in the age of 5 to 21 years. The dataset consists to a large proportion of children with a psychiatric disorder. For the 1644 downloaded EEG datasets full demographic data was available for 1609 subjects. 1415 of these 1609 subjects were diagnosed with a psychiatric disorder, while 194 subjects did not have any diagnosis. From these, 1485 could be used for further processing (mean age= 10.48, sd = 3.58, 506 female) due to incomplete data.

2.2. Experimental Setup and Procedure

The participant was comfortably seated in a chair in a sound- shielded room at a distance of 70 cm from a 17-inch CRT monitor (SONY Trinitron Multiscan G220, display dimensions 330 × 240 mm, resolution 800 × 600 pixels, vertical refresh rate of 100 Hz). The room was equipped with a chinrest to minimize head movements. Subjects were informed that EEG is recorded while they rest with their eyes alternately open or closed. Instructions for the tasks were presented on the computer screen, and a research assistant answered questions from the participant from the adjacent control room through an intercom. Compliance with the task instructions was confirmed through a live video-feed to the control room. The task procedure was that participants rest with their eyes open (EO) for 20 s (a total of 1 min 40 sec), followed

by 40 s (a total of 3 min 20 sec) with their eyes closed (EC), repeated five times. Pre-recorded verbal instructions informed the participants when to open or close their eyes automatically via loudspeakers. Participants were asked to maintain fixation on the fixation cross throughout EO blocks. The total duration of the EEG recording was 5 minutes. The alternating order of EO and EC blocks aimed at avoiding fatigue and maintaining vigilance. Moreover, the duration of EC blocks was intentionally twice as long as compared to EO blocks, because the focus of the resting state EEG analysis was on the eyes closed data as it is more robust and contains less artifacts. This protocol has been used in various previous studies (Langer et al., 2012; Langer, Bastian, Wirz, Oberauer, & Jäncke, 2013).

2.3. Electroencephalography Recording and Preprocessing

The EEG was recorded at a sampling rate of 500 Hz using a high-density 128-channel EEG Geodesic Netamps system (Electrical Geodesics, Eugene, Oregon). The recording reference was at Cz (vertex of the head), and impedances were kept below 40 kΩ. All analyses were performed using MATLAB 2018b (The MathWorks, Inc., Natick, Massachusetts, United States). EEG data was automatically preprocessed using the current version (2.4.3) of the MATLAB toolbox Automagic (Pedroni, Bahreini, & Langer, 2019). Our pipeline consisted of the following steps. First, 13 of 128 electrodes in the outermost circumference (chin and neck) were excluded from further processing as they capture little brain activity and mainly record muscular activity. Additionally, 10 EOG electrodes were separated from the data and not be used for further analysis, yielding in a total number of 105 EEG electrodes. Subsequently, bad channels were detected by the algorithms implemented in the eeglab plugin clean_rawdata (http://sccn.ucsd.edu/wiki/Plugin_list_process). A channel was defined as a bad electrode when recorded data from that electrode was correlated at less than 0.85 to an estimate based on other channels. Furthermore, a channel was defined as bad if it had more line noise relative to its signal than all other channels (4 standard deviations). Finally, if a channel had a longer flat-line than 5 s, it was considered bad. These bad channels were automatically removed and later interpolated using a spherical spline interpolation (EEGLAB function eeg_interp.m). The interpolation was performed as a final step before the automatic quality assessment of the EEG files (see below). Next, data was filtered using a high-pass filter (-6dB cut off: 0.5 Hz) and a 60Hz notch filter was applied to remove line noise artifacts. Subsequently, independent component analysis (ICA) was performed. Components reflecting artifactual activity were classified by the pre-trained classifier MARA (Winkler, Haufe, & Tangermann). Each component being classified with a probability rating >0.5 for any class of

artifacts was removed from the data. Finally, residual bad channels were excluded if their standard deviation exceeded a threshold of 25 μV. After this, the pipeline automatically assessed the quality of the resulting EEG files based on four criteria: First, a data file was marked as bad-quality EEG and not included in the analysis if the proportion of high-amplitude data points in the signals (>30 μV) was larger than 0.20. Second, more than 20% of time points showed a variance larger than 15 microvolt across channels. Third, 30% of the channels showed high variance (>15 μV). Fourth, the ratio of bad channels was higher than 0.3.

2.4. Spectral Analysis

Spectral analysis was performed on data from the concatenated five blocks of the eyes-closed condition. Only data from the eyes closed condition was analyzed, as this data contains fewer artifacts and generally shows the strongest alpha peaks. The first and the last second of each eyes-closed block was discarded to exclude motor activity related to opening and closing the eyes and auditory activity due to the prompt from the speakers. The remaining data was concatenated, resulting in a total of 190 seconds of continuous EEG data. This data was again segmented into 2 second epochs, each epoch containing large amplitude artifacts (> 90 μV, < - 90 μV), were excluded from further processing. On average, 2.95% of trials were excluded by this criterion. Power spectral densities (PSDs) were then calculated using Welch's Method (Welch, 1967) implemented in the EEGLab toolbox (Delorme & Makeig, 2004). Zero padding was be applied to provide a frequency resolution of 0.5 Hz in the 1 s sliding time windows within Welch's algorithm. Averaging the individual PSDs of each window results in a smoothed power spectrum that complies with the requirements of the FOOOF algorithm used subsequently (see below, Figure 1). Additionally, PSDs were transformed to log scale, to make results equally scaled to outputs from the FOOOF algorithm, which only operates in log power space. In the following, we describe the two approaches to extract total alpha power and the adjusted alpha power together with the aperiodic signal. See Table1 for an overview of all extracted parameters.

Table 1

Overview of extracted parameters

Parameter	Description
Individual alpha frequency (IAF)	Largest oscillatory peak detected by the FOOOF algorithm within range of 7 to 13.5 Hz
Total alpha peak power	Averaged log power in 1Hz window centered at IAF in total power spectrum
Total broadband alpha power	Averaged log power in window [- 4Hz + 2Hz] relative to IAF
Aperiodic adjusted alpha peak power	Height of the Gaussian reflecting the true alpha oscillation, as extracted by the FOOOF algorithm
Aperiodic intercept	Intercept parameter of the aperiodic signal extracted by FOOOF
Aperiodic slope	Slope exponent parameter of the aperiodic signal extracted by FOOOF

2.4.1. Computation of Individual Alpha Peak Frequency

To replicate the results of previous published findings, in this standard analysis approach, no adjustment for the aperiodic background signal was made. First, the individual alpha peak frequency (IAF) was found by extracting the oscillatory peaks, detected by the FOOOF algorithm (see below), between a lower and upper frequency limit. Following previous work, these frequencies limits were set to 7 and 13.5 Hz (Posthuma, Neale, Boomsma, & Geus, 2001; Smit, Wright, Hansell, Geffen, & Martin, 2006). If there was no peak within this window, no alpha peak was extracted for that subject and the corresponding data was excluded from further analysis (2.62% of the data, see also exclusion criteria in section 2.4.4).

2.4.2 Extraction of Total Alpha Power

If an alpha peak could be identified (see 2.4.1), total alpha peak power was extracted, by averaging log power within a 1 Hz window centered on the IAF. Additionally, a broader total alpha band power was calculated by averaging log power in the defined window [-4 Hz + 2 Hz] relative to the IAF (Klimesch, 1999). These individualized alpha power measures were chosen over a canonically defined alpha range (i.e. 8-13Hz), as the shift of the IAF during maturation might introduce a bias when power is averaged within a fixed frequency window.

2.4.3. FOOOF Algorithm and Aperiodic Adjusted Alpha Power

The FOOOF algorithm (Donoghue et al., 2020b) parameterizes the neural power spectrum to separate neural oscillations from the aperiodic background signal. The algorithm estimates oscillatory peaks that are superimposed on the aperiodic background signal (see Figure 1) and therefore measured relative to this rather than to the absolute zero. Consequently, the FOOOF algorithm parametrizes the PSD by iteratively fitting the aperiodic background curve (L) to the observed smoothed spectral signal, resulting in two parameters: the aperiodic intercept b and the aperiodic exponent χ (i.e. slope, the smaller χ, the flatter the spectrum).

$$L = b - \log(k + F^{\chi})$$

Here, F represents the vector of input frequencies and k the "knee" parameter, which is not further discussed here, as it is set to 0 in the proposed analysis (i.e. no bend of the aperiodic component is additionally modeled in the data, which is the default state of the FOOOF algorithm).

In order to extract oscillatory components, this aperiodic background signal is subtracted from the power spectrum. Gaussians are iteratively fitted to the remaining signal and subsequently subtracted whenever data points exceed two standard deviations of the data. The Gaussians represent the true oscillatory components in the data; if data points are below the specified threshold, they are considered as noise. This results in a data-driven number of Gaussians, each parameterized by the frequency center, power relative to the aperiodic signal and the frequency bandwidth. The power spectrum is therefore modeled by

$$P = L + \sum_{n=0}^{N} G_n + m\varepsilon,$$

where G_n represents the nth Gaussian, and m the scaling factor of the noise ε. Note that this description of the algorithm is simplified; for a more detailed definition, see Donoghue et al. (2020b).

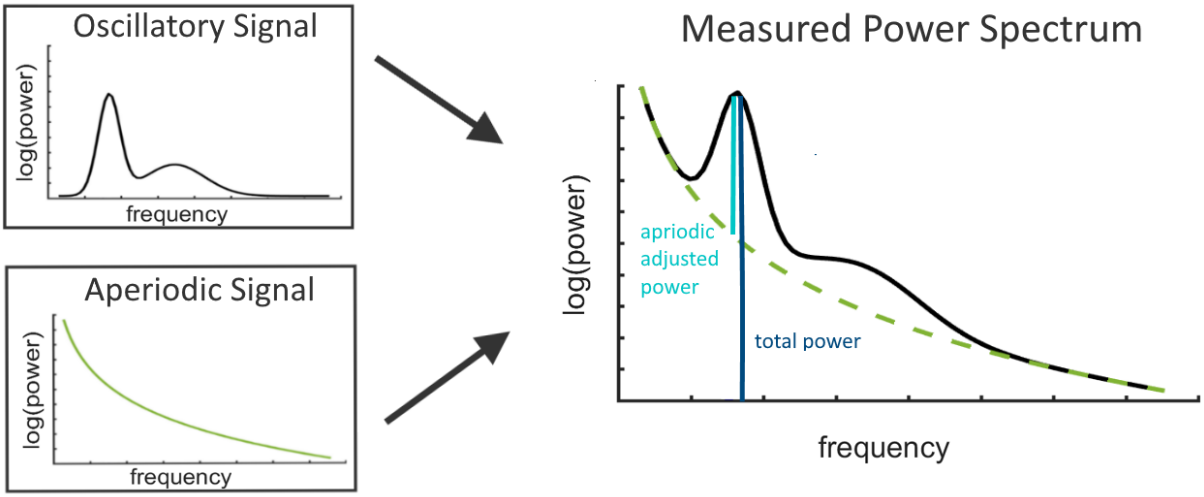

Figure 1: Illustration of a the different components superimposed in the measured neural power spectrum.

In the current study, the frequency range of 2 to 40 Hz of the power spectrum was passed to the algorithm because very low frequencies may lead to overfitting of noise as small bandwidth peaks. The current release (1.0.0) of the FOOOF toolbox from the github repository (https://github.com/fooof-tools/fooof) was used, applying standard peak detection parameters (2 standard deviations above mean). Gaussians within the alpha range of the alpha oscillation (7 - 13.5 Hz) were extracted for this analysis. If there were multiple Gaussians found, the one reflecting the oscillation with the highest power was taken as the individual alpha oscillation.

2.4.4. Cluster-wise Analysis

To test the hypothesis derived from literature review, an electrode-cluster-based analyses was performed. This cluster was based on data from the parietal and occipital electrodes, here referred to as the parieto-occipital cluster (see Figure 2). These electrodes were chosen because of the strong prominence of Oz and Pz electrodes in EEG alpha peak research (Klimesch, 1999) and previous findings for age effects on alpha band power in these electrodes (Clarke et al., 2001; Cragg et al., 2011; Gasser et al., 1988). To account for individual anatomical differences and to create a more robust cluster, electrodes adjacent to Oz and Pz were added (E54, E61, E67, E71, E75, E55, E62 , E72 , E79 , E78 , E77 , E76). All the parameters described above were averaged within the cluster. Before statistical analyses were performed, data was excluded if any the following criteria applied: The fit of the parameterized power spectrum to the original

PSD was below a cut-off of $R^2 < 0.9$. Any of the extracted parameters exceed a threshold of 3 standard deviations above or below the mean of the sample. No individual alpha peak could be detected.

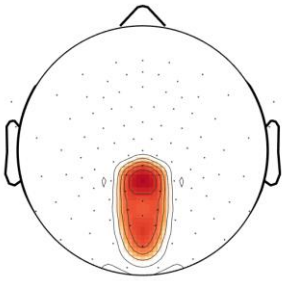

Figure 2: Visualization of the parieto-occipital cluster

Due to bad model fits (R^2 <.90) 0.41% of data points were excluded. Additionally, 4.68% of data points were excluded as they exceeded a threshold of three standard deviations in any of the parameters. In the remaining data, a high model fit over all posterior electrodes was observed for the parameterized power spectrum ($R^2_{\text{old}} = 0.993$, sd = 0.008). Finally, additional 2.62% of the available data were excluded as no alpha peak could be detected by the FOOOF algorithm. This yielded a final sample site of 1356 subjects.

2.5 Statistical Analysis

A Bayesian generalized linear mixed model was formulated using the brms R package (Bürkner, 2017). We chose a Bayesian approach over frequentist regression to be able to make inferences about the possible nonexistence of any effects. The model was defined as described in equation 1 and fitted to each dependent variable separately.

$$[dv] \sim age_{group}$$

The dependent variables were: IAF, total alpha peak power, total broadband alpha power, aperiodic adjusted alpha peak power, relative alpha power, aperiodic intercept and aperiodic slope (see table 1). All parameters were averaged within the above defined electrode clusters (see 2.4.4) and then passed to the statistical models.

To correct for multiplicity, the significance level (alpha) was adjusted. We assumed a high correlation between the 7 outcome variables, as many of the dependent variables represent different characteristics of the individual alpha oscillations. To account for this, we first calculated the effective number of tests of all dependent variables using Nyholt's approach (Nyholt, 2004). Following this approach, the significance level (0.05) was then adjusted using Šidák-Correction (Nyholt, 2004). Subsequently, the credible intervals (CIs) of the posterior distributions were calculated based on the newly estimated levels of significance. The resulting significance level was 0.01, yielding in 99% credible intervals. We refrained from calculating Bayes factors for point estimates (evidence for the effect to be zero / to be unequal to zero), as these Bayes factors (based on the Savage-Dickey ratio) heavily depend on the arbitrary choice of the prior distribution of each effect. Instead, we will consider a model parameter significant, if its 99% CI does not include zero.

In line with Gelman's recommendations (Gelman, Jakulin, Su, & Pittau, 2007), predictors and outcome variables of the Bayesian regression model were scaled as follows: The binary parameter (age) was centered at 0 and each numeric parameter (IAF, total alpha peak power, total broadband alpha power, aperiodic adjusted alpha peak power, relative alpha power, aperiodic intercept and aperiodic slope) was scaled to provide a mean of 0 and standard deviation 0.5. Uninformative Cauchy priors were used (mean=0, sd=2.5), as proposed by Gelman (Gelman et al., 2007).

3. Results

All relations of age to the various parameters estimated in the Bayesian regression model are visualized in Figure 3. These plots illustrate an increase in alpha peak frequency with increasing age. They further indicate a decrease of total alpha power parameters from childhood to adolescents. Importantly, this relationship inverses when alpha power is adjusted for the aperiodic signal, which then shows a similar age related trajectory as relative alpha power. Additionally, an age-related decrease of the aperiodic intercept and slope are indicated.

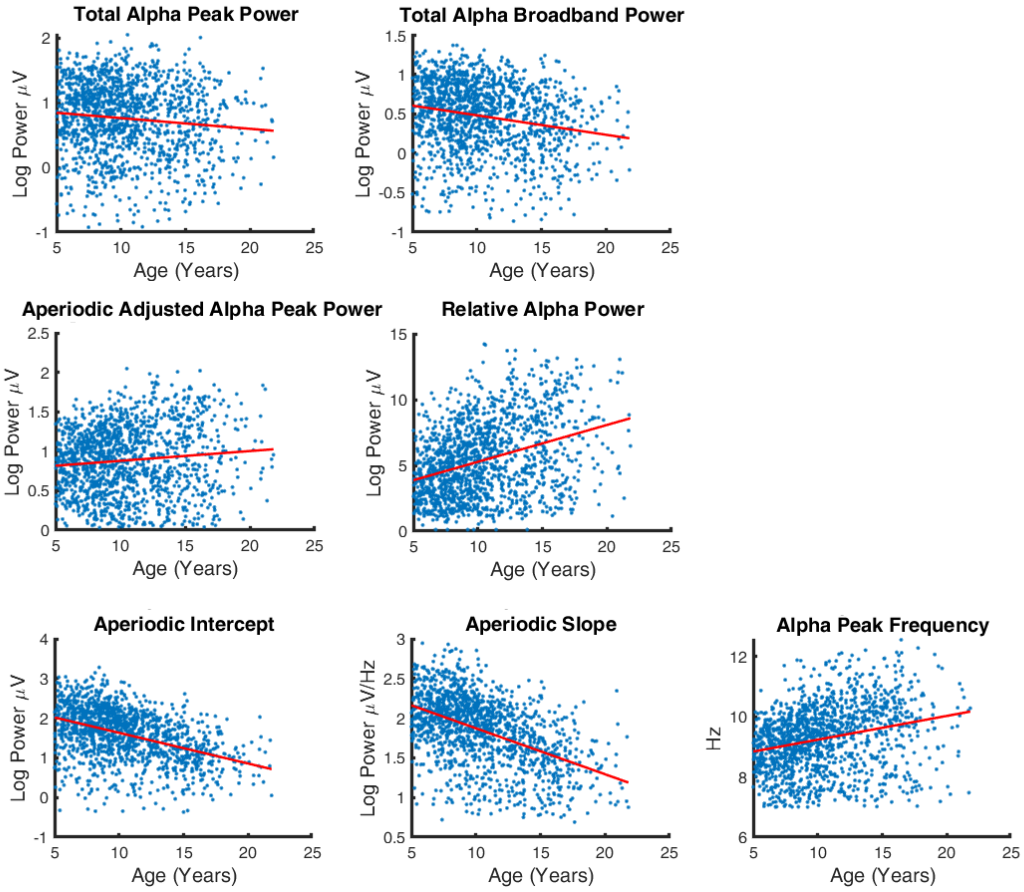

Figure 3: Visualization of data (blue) used in the Bayesian regression models. Red lines represent fitted regression lines.

The statistical model provided significant evidence for a reduction of total alpha peak power during brain maturation (*b*= -0.05, *99% CI*= [-0.08, -0.02]). Similar effects were observed for the total broadband alpha power (*b*= -0.10, *99% CI*= [-0.13, -0.07]). However when adjusting for the aperiodic signal, statistical results also imply a significant opposite age effect in the aperiodic adjusted alpha peak power (*b*= 0.06, *99% CI*= [0.03, 0.10]). This age effect shows the same direction as in relative alpha power (*b*=0.19, *99% CI*= [0.16 0.22]). As indicated above, aperiodic intercept (*b*= -0.24, *99% CI*= [-0.27, -0.21]) and slope (*b*= -0.25, *99% CI*= [-0.28, -0.22]) both significantly decreased with age, while the alpha peak frequency significantly increased (*b*= -0.10, *99% CI*= [0.10, 0.17]). Table 2 summarizes the results of the Bayesian regression model:

Table 2

Bayesian Regression Model Results

Parameter	Estimate	CI
Alpha peak frequency	0.13	[0.10 0.17]
Broadband alpha power	-0.10	[-0.13 -0.07]
Total alpha peak power	-0.05	[-0.08 -0.02]
Aperiodic adjusted alpha power	0.06	[0.03 0.10]
Relative alpha power	0.19	[0.16 0.22]
Aperiodic intercept	-0.24	[-0.27 -0.21]
Aperiodic slope	-0.25	[-0.28 -0.22]

Note: CI = 99% Credible Interval

Figure 4 shows the age related changes in the PSD during brain maturation. For visualization purposes, and in contrast to the statistical model, which used a continuous age variable, the sample was here split by the median (9.78 years) into a younger and older subsample. Panel A indicates a similar total alpha peak power between the two age groups, yet, in the statistical model, there was evidence for decrease with increasing continuous age (see above). Panel C visualizes the altered group differences when adjusting the power spectrum for the aperiodic signal. As previously described, the age differences in alpha peaks (power at ~10Hz) do clearly deviate from the differences visualized in panel A. The aperiodic signal itself shows a decreased intercept and flattened slope in age (see panel B).

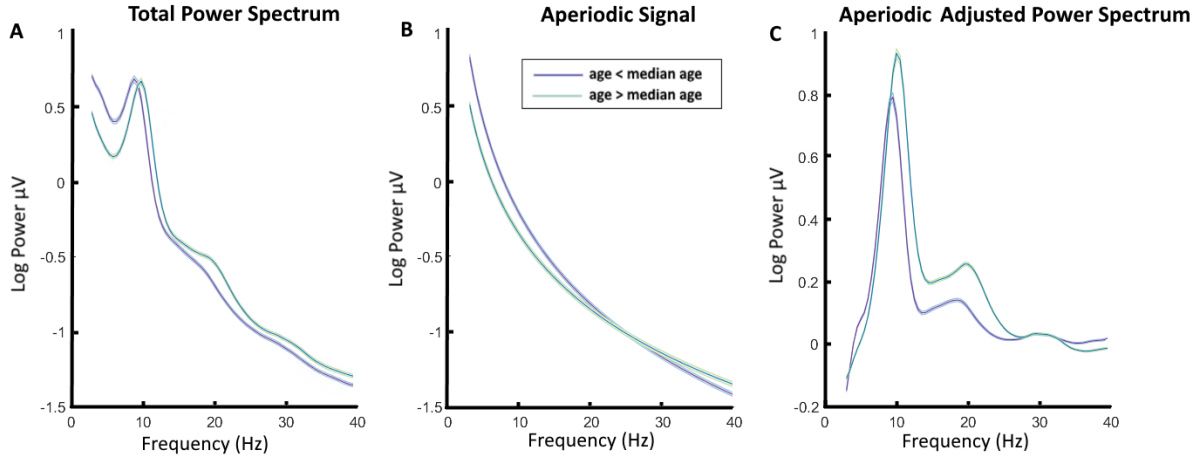

Figure 4: Visualization of changes in power spectrum during development: Averaged posterior spectral Power for each age group split by median. Total PSD signal (A) is separated into aperiodic signal (B) and aperiodic adjusted oscillatory power (C). Shaded error bars represent standard error of the mean. Note that statistical models used continuous age predictor.

3.1 Control Analysis

As the here investigated sample consists to a large proportion of children with a diagnosed psychiatric disorders, which might bias our finding on general brain maturation, we additionally subsampled the dataset and extracted only children without any diagnosed disorder (N= 180, mean age = 9.92 , sd=3.61, age range= 5 to 21 years, 87 female).

The same analysis is described above were applied to this sample. Table 3 summarizes the statistical results observed on this subsample. These results show large similarities with the results observed on the full sample. All parameters show the same relation to age, however, the aperiodic adjusted alpha power is no longer significantly associated with age.

Table 3

Bayesian Regression Model Results on Children without Psychiatric Diagnosis

Parameter	Estimate	CI
Alpha peak frequency	0.17	[0.08 0.27]
Broadband alpha power	-0.17	[-0.27 -0.07]
Total alpha peak power	-0.11	[-0.21 -0.01]
Aperiodic adjusted alpha power	0.05	[- 0.05 0.15]
Relative alpha power	0.15	[0.05 0.24]
Aperiodic intercept	-0.26	[-0.357 -0.17]
Aperiodic slope	-0.24	[-0.33 -0.15]

Note: CI = 99% Credible Interval

4. Discussion

The present study investigated the role of alpha oscillations during brain maturation. Our results replicated the well documented finding of an increasing individual alpha frequency in this developmental phase of life from childhood to adolescence. The main goal of the study was to clarify the developmental trajectory of the power of this alpha oscillation, considering aperiodic signal components and using a large sample size. A small, yet significant, decrease of total alpha power was overserved with increasing age. However, when correcting for the aperiodic signal, the results changed dramatically. Specifically, the aperiodic adjusted alpha power significantly increased with from childhood to adolescence. Interestingly, the same association was found for relative alpha power. The aperiodic signal itself showed a decreased intercept with increasing age during brain maturation, as well as a flattened slope.

The often replicated increase of IAF in the here investigated age range was also observed in the present analysis. A higher IAF is generally interpreted as increased speed of information processing or lower reaction times in cognitive tasks (Klimesch, 1999). This matches the findings of generally increased speed of information processing from childhood to adolescence (Kail, 2000).

The result of decreased total alpha power with increasing age is in line with previous studies which found this effect (Díaz de León et al., 1988; Gasser et al., 1988; Harmony et al., 1995; Whitford et al., 2007). It further indicates that the effect size of this age difference is very small. This is likely to be the reason why the evidence here is very mixed, as some other studies using smaller sample sizes than the present study were unable to find this association (Clarke et al., 2001; Somsen et al., 1997). Interestingly this effect changed its direction when adjusting for the aperiodic signal. This indicates that absolute band power measures are indeed conflated by changes in the aperiodic signal, as proposed by Donoghue et al. (2020b). The aperiodic signal in fact shows a general downshift with increasing age, which causes the absolute alpha power changes to appear negatively linked to age, although the true oscillatory power may increase with increasing age.

This also sheds light on the discrepancies in literature previously observed between total alpha power and relative alpha power (Clarke et al., 2001; Cragg et al., 2011; Díaz de León et al., 1988; Gasser et al., 1988; Harmony et al., 1995; Somsen et al., 1997; Whitford et al., 2007). When alpha power is calculated relative to the overall power, general shifts in the spectrum are subtracted out of the data, as it is also done in the aperiodic adjusted power. In the previous studies investigating relative alpha power, the relation of age with total alpha power was negative (i.e. decreasing during childhood and adolescence), while relative alpha power showed an increase during maturation. Our study replicated both of these previous findings, and additionally provides evidence for a downshift of the aperiodic signal and age-related increase in aperiodic adjusted alpha power. Combining these results suggests that the observed differences between total and relative alpha power may also at least partly be driven by changes the aperiodic signal.

The decrease of the aperiodic intercept replicates previous observations (Donoghue, Dominguez, & Voytek, 2020a; He, 2014). While on study (Donoghue et al., 2020a) investigated a correlation across the age range from 6 to 44, which is beyond the here investigated sample, the other study (He et al., 2019) found a decrease between the young and the adult group and also within the young subsample. The present analysis further indicates that this decrease is evident within the process of brain maturation during childhood and adolescence. As previous studies could show that the aperiodic intercept reflects the overall spiking activity of the underlying neural population (Miller et al., 2009) the present study indicates a decreased spiking activity during brain maturation measured by parieto-occipital electrodes. The underlying mechanism for this observation may lie within the finding that as much as about 40% of synapses in the striate cortex, which are captured by the here

investigated electrodes, are eliminated during brain development (Huttenlocher & Courten, 1987). An alternative interpretation of this decrease of the aperiodic intercept could be given by Ohm's law, as maturation is accompanied by thickening of the skull, leading in higher resistance and thus generally lower amplitudes in the EEG signal. He et al. (2019) used MEG, which is not affected by the thickness of the skull. As described above, they could still find a decrease of the aperiodic intercept within the young group, yet this needs to be interpreted with caution due to the small subsample of young subjects (N=24). More research is needed to clarify this association.

The flattening of the aperiodic signal (i.e. absolute decrease of the aperiodic slope) during brain development is in line with previous findings (He et al., 2019). Furthermore, this may also reflect the previously typically observed age related decrease of power in low frequencies accompanied by an increase in power in higher frequencies in this age range (Cragg et al., 2011; Whitford et al., 2007). Underlying mechanisms were speculated within the elimination of synapses or changes in white matter structure (Segalowitz, Santesso, & Jetha, 2010; Whitford et al., 2007). Taking changes in the aperiodic slope into account could provide additional insights into this so far not fully understood result. A flattening of the aperiodic signal has previously been linked to increased neural noise and a decorrelation of activity in underlying neural populations (Voytek & Knight, 2015). The here observed flattened slope might thus reflect earlier findings on increases in neural noise during brain development (for a review, see McIntosh, 2010). Reviewing maturational studies using EEG and functional magnetic resonance imaging, the authors concluded that the maturing brain is developing from a deterministic to a more stochastic system, in which the increased neural noise leads to enhancement of functional network potential. Following the argumentation He et al. (2019), the flattened aperiodic signal in brain maturation might also reflect the reduction of autocorrelation of the time series EEG data. This reduction of autocorrelation was then associated with the increased demand in working memory tasks to efficiently process information during cognitive load (He, 2014).

Taken together, this study has shown the importance of taking aperiodic signal components into account when investigating age related changes of spectral power during brain maturation. Our results indicate that differences in the aperiodic signal may have been mistaken as differences in total alpha power in previous literature. Thus, interpretations of these oscillatory changes should be done with caution and incorporate changes in the aperiodic signal. Furthermore, the direction of the age effect on true oscillatory alpha power seems to be opposite as previously assumed when investigating total alpha power.

A limitation of the present study is the composition of the investigated sample, as it contains a large proportion of children with diagnosed psychiatric disorders. Yet, control analyses using only a healthy subsample show very similar results, although the sample size is very limited here compared to the full sample.

References

Alexander, L. M., Escalera, J., Ai, L., Andreotti, C., Febre, K., Mangone, A., et al. (2017). An open resource for transdiagnostic research in pediatric mental health and learning disorders. *Scientific data, 4*, 170181.

Bürkner, P.-C. (2017). *Advanced Bayesian Multilevel Modeling with the R Package brms*, from http://arxiv.org/pdf/1705.11123v2.

Clarke, A. R., Barry, R. J., McCarthy, R., & Selikowitz, M. (2001). Age and sex effects in the EEG: development of the normal child. *Clinical Neurophysiology, 112*(5), 806–814, from http://www.sciencedirect.com/science/article/pii/S1388245701004886.

Cragg, L., Kovacevic, N., McIntosh, A. R., Poulsen, C., Martinu, K., Leonard, G., & Paus, T. (2011). Maturation of EEG power spectra in early adolescence: a longitudinal study. *Developmental science, 14*(5), 935–943, from https://pubmed.ncbi.nlm.nih.gov/21884309/.

Delorme, A., & Makeig, S. (2004). EEGLAB: an open source toolbox for analysis of single-trial EEG dynamics including independent component analysis. *Journal of neuroscience methods, 134*(1), 9–21.

Díaz de León, A. E., Harmony, T., Marosi, E., Becker, J., & Alvarez, A. (1988). Effect of different factors on EEG spectral parameters. *The International journal of neuroscience, 43*(1-2), 123–131.

Donoghue, T., Dominguez, J., & Voytek, B. (2020a). Electrophysiological Frequency Band Ratio Measures Conflate Periodic and Aperiodic Neural Activity. *eNeuro*.

Donoghue, T., Haller, M., Peterson, E., Varma, P., Sebastian, P., Gao, R., et al. (2020b). Parameterizing neural power spectra into periodic and aperiodic components. *Nature neuroscience, in press*.

Foxe, J. J., & Snyder, A. C. (2011). The Role of Alpha-Band Brain Oscillations as a Sensory Suppression Mechanism during Selective Attention. *Frontiers in psychology, 2*, 154.

Gasser, T., Verleger, R., Bächer, P., & Sroka, L. (1988). Development of the EEG of school-age children and adolescents. I. Analysis of band power. *Electroencephalography and Clinical Neurophysiology, 69*(2), 91–99.

Gelman, A., Jakulin, A., Su, Y.-S., & Pittau, M. G. (2007). A Default Prior Distribution for Logistic and Other Regression Models. *SSRN Electronic Journal*.

Giedd, J. N., Blumenthal, J., Jeffries, N. O., Castellanos, F. X., Liu, H., Zijdenbos, A., et al. (1999). Brain development during childhood and adolescence: a longitudinal MRI study. *Nature neuroscience, 2*(10), 861–863.

Harmony, T., Marosi, E., Becker, J., Rodríguez, M., Reyes, A., Fernández, T., et al. (1995). Longitudinal quantitative EEG study of children with different performances on a reading-writing test. *Electroencephalography and Clinical Neurophysiology, 95*(6), 426–433.

He, B. J. (2014). Scale-free brain activity: past, present, and future. *Trends in cognitive sciences, 18*(9), 480–487.

He, W., Donoghue, T., Sowman, P. F., Seymour, R. A., Brock, J., Crain, S., et al. (2019). *Co-Increasing Neuronal Noise and Beta Power in the Developing Brain.*

Huttenlocher, P. R., & Courten, C. de (1987). The development of synapses in striate cortex of man. *Human neurobiology, 6*(1), 1–9.

John, E. R., Ahn, H., Prichep, L., Trepetin, M., Brown, D., & Kaye, H. (1980). Developmental equations for the electroencephalogram. *Science (New York, N.Y.), 210*(4475), 1255–1258, from https://pubmed.ncbi.nlm.nih.gov/7434026/.

Kail, R. (2000). Speed of Information Processing. *Journal of School Psychology, 38*(1), 51–61.

Kessler, R. C., Berglund, P., Demler, O., Jin, R., Merikangas, K. R., & Walters, E. E. (2005). Lifetime prevalence and age-of-onset distributions of DSM-IV disorders in the National Comorbidity Survey Replication. *Archives of general psychiatry, 62*(6), 593–602.

Klimesch, W. (1997). EEG-alpha rhythms and memory processes. *International Journal of Psychophysiology, 26*(1-3), 319–340.

Klimesch, W. (1999). EEG alpha and theta oscillations reflect cognitive and memory performance: a review and analysis. *Brain Research Reviews, 29*(2-3), 169–195.

Klimesch, W. (2012). α-band oscillations, attention, and controlled access to stored information. *Trends in cognitive sciences, 16*(12), 606–617, from http://www.sciencedirect.com/science/article/pii/S1364661312002434.

Langer, N., Bastian, C. C. von, Wirz, H., Oberauer, K., & Jäncke, L. (2013). The effects of working memory training on functional brain network efficiency. *Cortex; a journal devoted to the study of the nervous system and behavior, 49*(9), 2424–2438, from http://www.sciencedirect.com/science/article/pii/S0010945213000117.

Langer, N., Pedroni, A., Gianotti, L. R. R., Hänggi, J., Knoch, D., & Jäncke, L. (2012). Functional brain network efficiency predicts intelligence. *Human brain mapping, 33*(6), 1393–1406.

Lebel, C., Walker, L., Leemans, A., Phillips, L., & Beaulieu, C. (2008). Microstructural maturation of the human brain from childhood to adulthood. *NeuroImage, 40*(3), 1044–1055.

Markand, O. N. (1990). Alpha rhythms. *Journal of Clinical Neurophysiology, 7*(2), 163–190.

McIntosh, A. R. (2010). The Development of a Noisy Brain. *Archives Italiennes de Biologie*. (148), 223–337.

Miller, K. J., Sorensen, L. B., Ojemann, J. G., & den Nijs, M. (2009). Power-law scaling in the brain surface electric potential. *PLoS computational biology, 5*(12), e1000609.

Niedermeyer, E. (1999). The normal EEG of the waking adult. *Electroencephalography: Basic principles, clinical applications, and related fields, 167*, 155–164.

Nyholt, D. R. (2004). A simple correction for multiple testing for single-nucleotide polymorphisms in linkage disequilibrium with each other. *American journal of human genetics, 74*(4), 765–769.

Pedroni, A., Bahreini, A., & Langer, N. (2019). Automagic: Standardized preprocessing of big EEG data. *NeuroImage*, 460–473.

Posthuma, D., Neale, M. C., Boomsma, D. I., & Geus, E. J. de (2001). Are smarter brains running faster? Heritability of alpha peak frequency, IQ, and their interrelation. *Behavior genetics, 31*(6), 567–579.

Segalowitz, S. J., Santesso, D. L., & Jetha, M. K. (2010). Electrophysiological changes during adolescence: a review. *Brain and cognition, 72*(1), 86–100.

Smit, C. M., Wright, M. J., Hansell, N. K., Geffen, G. M., & Martin, N. G. (2006). Genetic variation of individual alpha frequency (IAF) and alpha power in a large adolescent twin sample. *International journal of psychophysiology : official journal of the International Organization of Psychophysiology, 61*(2), 235–243, from http://www.sciencedirect.com/science/article/pii/S0167876005002618.

Somsen, R. J., van't Klooster, B. J., van der Molen, M. W., van Leeuwen, H. M., & Licht, R. (1997). Growth spurts in brain maturation during middle childhood as indexed by EEG power spectra. *Biological Psychology, 44*(3), 187–209.

Usher, Stemmler, & Olami (1995). Dynamic pattern formation leads to 1/f noise in neural populations. *Physical review letters, 74*(2), 326–329.

Voytek, B., & Knight, R. T. (2015). Dynamic network communication as a unifying neural basis for cognition, development, aging, and disease. *Biological psychiatry, 77*(12), 1089–1097.

Welch, P. (1967). The use of fast Fourier transform for the estimation of power spectra: A method based on time averaging over short, modified periodograms. *IEEE Transactions on Audio and Electroacoustics, 15*(2), 70–73.

Whitford, T. J., Rennie, C. J., Grieve, S. M., Clark, C. R., Gordon, E., & Williams, L. M. (2007). Brain maturation in adolescence: concurrent changes in neuroanatomy and neurophysiology. *Human brain mapping, 28*(3), 228–237.

Winkler, I., Haufe, S., & Tangermann, M. Automatic classification of artifactual ICA-components for artifact removal in EEG signals, *2011*(7), 30.